Relationship between left coronary artery bifurcation angle and restenosis after stenting of the proximal left anterior descending artery

Takao Konishi[a,b], Tadashi Yamamoto[a], Naohiro Funayama[a], Hiroshi Nishihara[b] and Daisuke Hotta[a]

Introduction **Restenosis after a percutaneous coronary intervention for proximal left anterior descending (pLAD) coronary artery disease remains a clinical challenge. However, the relationship between the left main trunk (LMT)/LAD bifurcation angle and the pLAD artery restenosis is unclear. This study examined the relationship between the LMT–LAD bifurcation angle and restenosis after stent implantation for pLAD disease.**

Methods **We analysed the data of 177 consecutive patients who underwent stent implantation for pLAD disease, followed by coronary angiography between December 2008 and September 2013. The LMT–LAD bifurcation angle was measured in the left or the right anterior oblique caudal (CAU) angiographic view.**

Results and discussion **Out of 177 patients, 12 developed in-stent restenosis and 21 developed in-segment restenosis. The mean angle in patients with in-stent restenosis (52.2° ± 14.5°) in the left anterior oblique CAU view was significantly larger than that in patients without restenosis (32.0° ± 18.1°; $P < 0.001$). The LMT–LAD angle in the right anterior oblique CAU view was significantly larger in patients with in-segment restenosis (27.3° ± 14.3°) than in patients without restenosis (17.5° ± 10.1°; $P < 0.001$). Moreover, by multivariate analysis, the LMT–LAD angle was an independent predictor of in-stent and in-segment restenosis, after adjustment for significant confounders such as diabetes, hypertension, dyslipidaemia, final minimum lesion diameter and lesion length.**

Conclusion **This study suggests that a wide LMT–LAD angle is a predictor of restenosis after stent implantation for pLAD artery disease.** ***Coron Artery Dis*** **27:449–459**

Coronary Artery Disease 2016, **27**:449–459

Keywords: coronary restenosis, coronary stent, left coronary angle, left coronary bifurcation, percutaneous coronary intervention

[a]Department of Cardiology, Hokkaido Cardiovascular Hospital and [b]Department of Translational Pathology, Hokkaido University School of Medicine, Sapporo, Japan

Correspondence to Takao Konishi, MD, Department of Cardiology, Hokkaido Cardiovascular Hospital, 1-30, West 13, South 27, Chuou-ku, Sapporo 064-8622, Japan
Tel: +81 11 563 3911; fax: +81 11 551 3109;
e-mail: takaokonishi0915@gmail.com

Received 4 February 2016 **Revised** 12 March 2016 **Accepted** 11 April 2016

Introduction

Drug-eluting stents represent considerable progress in the percutaneous treatment of coronary artery disease. However, restenosis of stents implanted in the proximal left anterior descending (pLAD) artery remains a clinical challenge. As the pLAD artery supplies ~50% of the left ventricular myocardial blood flow [1,2], its occlusion is often associated with worse outcomes than the occlusion of other epicardial coronary arteries [3], and percutaneous coronary interventions (PCI) on the pLAD are associated with a higher risk of complications than on any other location [2,4,5]. Despite the absence of significant differences in the incidence of myocardial infarction and death associated with coronary artery bypass graft (CABG) versus PCI [3,6,7], the latter is followed by a higher incidence of repeat revascularization of the pLAD artery than the former [6–12]. Consequently, whether PCI or CABG is preferable for patients presenting with pLAD artery disease remains controversial. According to the 2011 guidelines issued by the American College of Cardiology Foundation, the American Heart Association and the Society for Cardiovascular Angiography and Interventions, the grade recommended for the treatment of pLAD artery disease is lower for PCI than for CABG [13]. Therefore, when performing PCI for pLAD artery disease, the risks of postprocedural stent restenosis must be acknowledged and evaluated with particular care. Several factors have been identified in population-based studies, which increase the risk of stent restenosis, including diabetes, stent length and final minimal lumen diameter (MLD) [14]. The angle between the left main trunk (LMT) and the LAD artery, however, has not been described.

Supplemental digital content is available for this article. Direct URL citations appear in the printed text and are provided in the HTML and PDF versions of this article on the journal's website (*www.coronary-artery.com*).

0954-6928 Copyright © 2016 Wolters Kluwer Health, Inc. All rights reserved.

DOI: 10.1097/MCA.0000000000000381

As the mechanism of stent restenosis is different in stented versus nonstented lesions [15], we separately classified 'in-stent' from 'in-segment' when searching for factors of risk of restenosis and hypothesized that the angulation between LMT and LAD artery has an influence on the development of in-stent or in-segment restenosis, or both. This study examined whether the bifurcation angle of the LAD artery is related to the incidence of restenosis after stent implantation for pLAD artery disease.

Methods

Sample population

We analysed the data from 1446 consecutive patients who underwent PCI between December 2008 and September 2013 at Hokkaido Cardiovascular Hospital, Japan. A total of 250 patients underwent stent implantation of the pLAD artery and 177 underwent a follow-up angiography. All patients with stent implantation of the pLAD artery were included irrespective of the distance from the left main bifurcation. We excluded patients who had undergone only balloon angioplasty or had had crossover stenting from the LAD artery to the LMT. The factors that we chose as potential factors of risk of restenosis are listed in the Appendix. Restenosis was defined as at least 50% luminal narrowing on two-dimensional quantitative coronary angiography (QCA) using Stenosis Analysis, version 1.6.259 (GE Medical Systems S.C.S., Buc, France). In-stent restenosis was defined as any luminal narrowing inside the stented segment. In-segment restenosis was defined as any luminal narrowing within 5 mm proximal or distal from the stent edge. This study was approved by an institutional review committee and the patients provided informed consent.

Angles of bifurcations

The left anterior oblique caudal (LAO/CAU) or Spider view is the most effective for visualization of the LMT bifurcation to the LAD and left circumflex (LCX) arteries. As the optimal view of the LMT bifurcation is usually between the LAO and right anterior oblique (RAO) CAU projections [16], we studied the LMT–LAD angles in the Spider and RAO/CAU views and the LAD–LCX and LMT–LCX angles in the Spider view. These angles of preprocedure were measured three times on end-diastolic frames and the average angles were calculated. The measurements of each angle are shown in Fig. 1 and examples of no restenosis and restenosis are shown in Fig. 2. In this study, the Spider view was in a LAO 44.2° ± 1.0°, caudal 32.5° ± 2.0° projection, and the RAO/CAU view was in a RAO 30.0° ± 0.9°, caudal 22.0° ± 2.5° projection. The mean viewing angles of the no-restenosis, in-stent restenosis and in-segment restenosis groups were similar (data not shown).

Definitions

Diabetes mellitus was defined as (a) plasma glucose of at least 126 mg/dl in the fasting state, or (b) at least 200 mg/dl, 2 h after an oral glucose load, or (c) at least 6.5% plasma haemoglobin A1c, or (d) use of insulin or an oral hypoglycaemic agent. Hypertension was defined as at least 140 mmHg systolic blood pressure, at least 90 mmHg diastolic blood pressure or use of an antihypertensive drug. Dyslipidaemia was defined as at least 220 mg/dl total cholesterol, at least 140 mg/dl low-density lipoprotein cholesterol, high-density lipoprotein cholesterol, at least 150 mg/dl triglyceride or the use of a blood lipid-lowering drug. Chronic kidney disease (CKD) was defined as an estimated glomerular filtration rate of less than 60 ml/min/1.73 m^2 for at least 3 months. A bending lesion was defined as a lesion that has a greater than 60° angulation.

Statistical analysis

The data are expressed as means ± SD. Between-group differences were examined using Student's *t*-test for continuous variables and χ^2-test or Fisher exact test for categorical variables. Univariate and multivariate logistic regression analyses were carried out to identify independent factors of risk of total, in-stent and in-segment restenoses. The risk factors for each type of restenosis were identified using univariate and multivariate logistic regression models that included predictors of restenosis by univariate analysis and factors associated with restenotic events in previous publications. Male sex, diabetes, hypertension, dyslipidaemia, CKD, bare-metal stent use, chronic total occlusion, distance between the ostium of the LAD and the proximal edge of the stent, final MLD, high-degree calcification, lesion length, LMT–LAD angle (Spider view) and LMT–LCX angle (Spider view) were entered into the multivariate model. We then entered the LAD–LCX angle (Spider view) or the LMT–LAD angle (RAO/CAU view) in the multivariate model instead of the LMT–LAD angle (Spider view) and compared these. Odds ratio (OR) and 95% confidence intervals (CIs) were calculated to ascertain the significance of the differences. A *P*-value of less than 0.05 was considered statistically significant. The data were analysed using the SPSS 19.0 statistical system software (IBM Corporation, Armonk, New York, USA).

Results

Clinical observations

The mean follow-up duration was 11.2 ± 6.5 months in the overall population, 11.3 ± 10.9 months in the no-restenosis group and 12.3 ± 23.3 months in the restenosis group (NS). During this period, a pLAD artery restenosis was found in 33 of 177 patients (18.6%), of whom 12 had an in-stent restenosis and 21 patients had an in-segment restenosis. The baseline patient characteristics are listed in Table 1. The mean age of the patients in the two study groups was similar. A higher prevalence of dyslipidaemia

Fig. 1

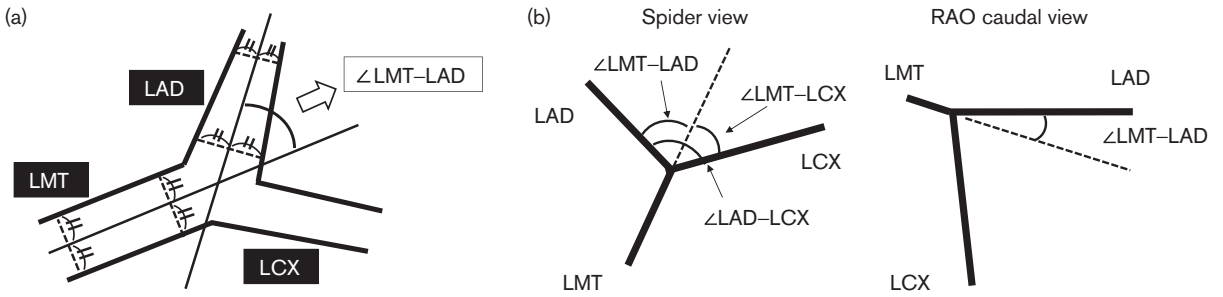

(a) Determination of the lines that yielded the angle of interest, taking for example the LMT–LAD angle in the Spider view. We used the centreline of the coronary angiogram. (b) Measurements of angles. The LMT bifurcation angle was measured in the Spider and the RAO caudal views. LAD, left anterior descending; LCX, left circumflex; LMT, left main trunk; RAO, right anterior oblique.

Fig. 2

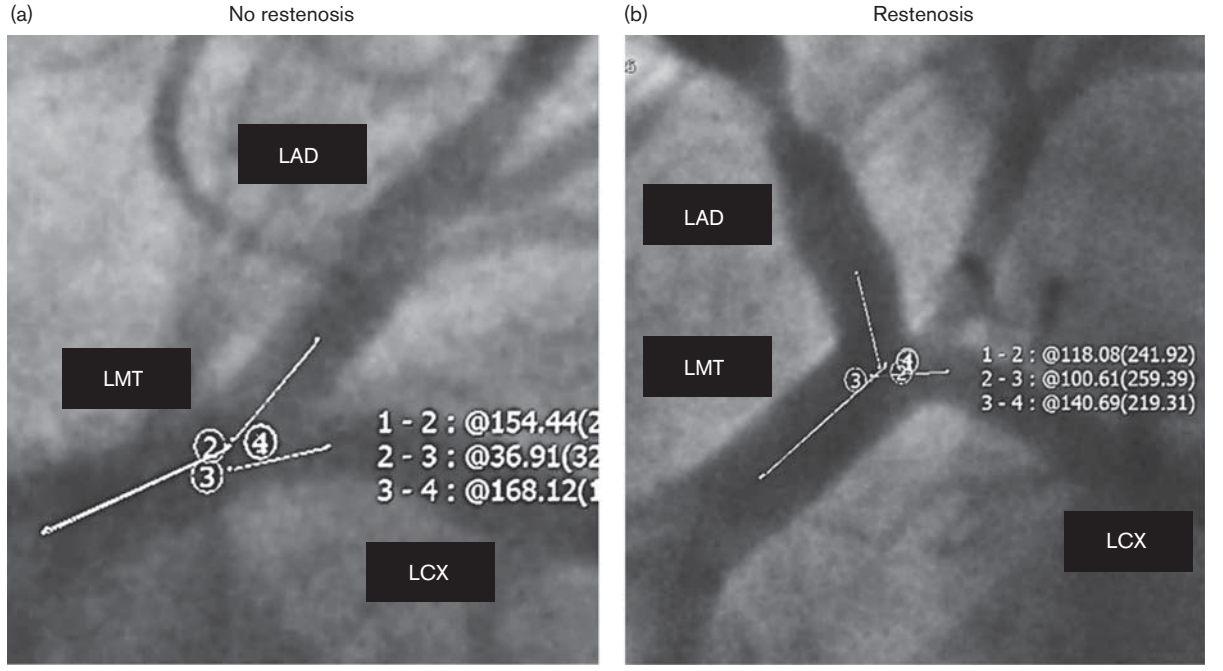

Representative examples of no restenosis and restenosis. (a) The LMT–LAD angle in the Spider view measured 25.6° in a 69-year-old man with no restenosis in the pLAD artery; (b) in another 70-year-old man, the angle measured 61.9° with a restenotic pLAD artery lesion. LAD, left anterior descending; LCX, left circumflex; LMT, left main trunk; pLAD, proximal left anterior descending.

was observed in the no-restenosis group (87.5%) than in the restenosis (72.7%) group ($P = 0.033$). All other clinical characteristics were similar in both groups. The adherence to dual antiplatelet therapy with aspirin and clopidogrel or ticlopidine after stent implantation was 95.8% in the no-restenosis group and 93.9% in the restenosis group (NS).

Lesions, procedural and anatomical characteristics

The lesion, procedural and anatomical characteristics are shown in Table 2. The distance between the ostium of the LAD and the proximal edge of the stent was significantly longer and the final MLD was significantly smaller in the restenosis group than in the no-restenosis group. The LMT–LAD angle and the LAD–LCX angle in Spider view and the LMT–LAD angle in the RAO/CAU view were significantly wider in the restenosis group than in the no-restenosis group. The LMT–LCX angle in Spider view was similar in both the restenosis and the no-restenosis group.

We further divided the restenosis group into in-stent and in-segment restenosis groups. The characteristics of in-

Table 1 Baseline characteristics of no-restenosis and restenosis groups

	No restenosis ($N=144$)	Restenosis ($N=33$)	P
Age at the time of stenting (years)	67.4±10.1	68.2±10.3	0.687
Men	110 (76.4)	27 (81.8)	0.501
Canadian Cardiovascular Society classification	2.67±1.26	2.58±1.30	0.710
Acute coronary syndrome	65 (45.1)	13 (39.4)	0.549
Diabetes	56 (38.9)	18 (54.5)	0.100
Hypertension	120 (83.3)	29 (87.9)	0.519
Dyslipidaemia	126 (87.5)	24 (72.7)	0.033
Chronic kidney disease	40 (27.8)	14 (42.4)	0.099
Left ventricular ejection fraction	59.3±9.3	57.4±11.5	0.382
Statin	118 (81.9)	22 (66.7)	0.052
Aspirin	137 (95.1)	32 (97.0)	0.994
Ticlopidine	25 (17.4)	5 (15.2)	0.760
Clopidogrel	114 (79.2)	27 (81.8)	0.733
Dual antiplatelet therapy	138 (95.8)	31 (93.9)	0.994

Values are means±SD or numbers (%) of observations.

Table 2 Lesion, procedural and anatomical characteristics of no-restenosis and restenosis groups

	No restenosis ($N=144$)	Restenosis ($N=33$)	P
Bare-metal stent	27 (18.8)	7 (21.2)	0.746
Stent diameter (mm)	3.4±0.3	3.3±0.4	0.113
Total stent length (mm)	22.5±9.6	25.5±9.4	0.104
Chronic total occlusion	6 (4.2)	3 (9.1)	0.470
Stenosis severity	91.1±9.2	89.7±10.1	0.455
Distance between the ostium of LAD and the proximal edge of the stent (mm)	5.2±5.1	8.0±5.7	0.007
Final minimum lumen diameter (mm)	3.0±0.3	2.5±0.6	<0.001
High-degree calcification	11 (7.6)	6 (18.2)	0.064
Lesion length (mm)	17.8±11.5	18.2±9.9	0.822
Lesion angulation >60°	4 (2.8)	0 (0)	0.750
Diagonal branch	83 (57.6)	22 (66.7)	0.341
Predilatation	118 (81.9)	29 (87.9)	0.574
Postdilatation	60 (41.7)	13 (39.4)	0.811
Kissing balloon technique	4 (2.8)	2 (6.1)	0.684
Intravascular ultrasound	137 (95.1)	30 (90.9)	0.595
Angles (deg.)			
Left main trunk–left anterior descending (Spider view)	32.0±18.1	43.5±18.2	0.001
Left main trunk–left circumflex (Spider view)	43.4±20.7	40.5±17.7	0.422
Left anterior descending–left circumflex (Spider view)	75.4±24.5	84.0±23.6	0.040
Left main trunk–left anterior descending (RAO/CAU view)	17.5±10.1	28.9±14.0	<0.001

Values are means±SD or numbers (%) of observations.
CAU, caudal; LAD, left anterior descending; RAO, right anterior oblique.

stent restenosis are shown in Table 3. Significant risk factors for in-stent restenosis were a narrower final MLD, a longer lesion length and a wider LMT–LAD angle in Spider view, LAD–LCX angle in Spider view and LMT–LAD angle in RAO/CAU view.

Table 4 shows the characteristics of in-segment restenosis. Significant risk factors for in-segment restenosis were dyslipidaemia, a longer distance between the ostium of the LAD and the proximal edge of the stent, and a wider LMT–LAD angle (RAO/CAU).

Table 3 Characteristics of the no-restenosis group versus the in-stent restenosis group

	No restenosis ($N=144$)	In-stent restenosis ($N=12$)	P
Age at coronary stenting (years)	67.4±10.1	68.8±10.6	0.649
Men	110 (76.4)	10 (83.3)	0.848
Canadian Cardiovascular Society classification	2.7±1.3	3.3±1.1	0.077
Acute coronary syndrome	65 (45.1)	8 (66.7)	0.256
Diabetes	56 (38.9)	6 (50.0)	0.450
Hypertension	120 (83.3)	9 (75.0)	0.737
Dyslipidaemia	126 (87.5)	10 (83.3)	0.972
Chronic kidney disease	40 (27.8)	6 (50.0)	0.105
Left ventricular ejection fraction	59.3±9.3	54.7±11.3	0.195
Statin	118 (81.9)	9 (75.0)	0.835
Aspirin	137 (95.1)	12 (100)	0.955
Ticlopidine	25 (17.4)	3 (25.0)	0.786
Clopidogrel	114 (79.2)	9 (75.0)	0.977
Dual antiplatelet therapy	138 (95.8)	12 (100)	0.952
Bare-metal stent	27 (18.8)	4 (33.3)	0.401
Stent diameter (mm)	3.4±0.3	3.3±0.3	0.249
Total stent length (mm)	22.5±9.6	25.8±7.5	0.180
Chronic total occlusion	6 (4.2)	1 (8.3)	0.955
Stenosis severity	91.1±9.2	90.3±10.2	0.789
Distance between the ostium of the LAD and the proximal edge of the stent (mm)	5.2±5.1	5.8±3.7	0.590
Final minimum lumen diameter (mm)	3.0±0.3	2.5±0.6	0.007
High-degree calcification	11 (7.6)	2 (16.7)	0.587
Lesion length (mm)	17.8±11.5	22.9±6.4	0.026
Lesion angulation >60°	4 (2.8)	0 (0)	0.715
Diagonal branch	83 (57.6)	9 (75.0)	0.385
Predilatation	118 (81.9)	11 (91.7)	0.647
Postdilatation	60 (41.7)	5 (41.7)	1.000
Kissing balloon technique	4 (2.8)	0 (0)	0.715
Intravascular ultrasound	137 (95.1)	11 (91.7)	0.875
Angles (deg.)			
Left main trunk–left anterior descending (Spider view)	32.0±18.1	52.2±14.5	<0.001
Left main trunk–left circumflex (Spider view)	43.4±20.7	41.9±10.5	0.681
Left anterior descending–left circumflex (Spider view)	75.4±24.5	94.1±18.6	0.007
Left main trunk–left anterior descending (RAO/CAU view)	17.5±10.1	31.6±13.7	<0.001

Values are means±SD or numbers (%) of observations.
CAU, caudal; LAD, left anterior descending; RAO, right anterior oblique.

We compared the prevalence of each risk factor in the presence of no restenosis and in the presence of in-stent versus in-segment restenosis (Fig. 1a–h, Supplemental digital content 1, *http://links.lww.com/MCA/A74*). Dyslipidaemia was most prevalent in the no-restenosis group and was similar in both restenosis groups, whereas the final MLD was significantly wider in the no-restenosis group than in both the in-stent and the in-segment restenosis groups. The distance between the ostium of the LAD and the proximal edge of the stent was significantly longer in the in-segment restenosis than in the no-restenosis group, whereas the mean lesion length was significantly longer in the in-stent restenosis than in both the other groups. The mean LMT–LAD angle (Spider view) was wider in both restenosis groups than in the no-restenosis group. The mean LMT–LCX

Table 4 Characteristics of no restenosis versus in-segment restenosis

	No restenosis ($N=144$)	In-segment restenosis ($N=21$)	P
Age at the time of stenting (years)	67.4 ± 10.1	67.8 ± 10.4	0.850
Men	110 (76.4)	17 (81.0)	0.852
Canadian Cardiovascular Society classification	2.7 ± 1.3	2.1 ± 1.2	0.076
Acute coronary syndrome	65 (45.1)	5 (23.8)	0.065
Diabetes	56 (38.9)	12 (57.1)	0.112
Hypertension	120 (83.3)	20 (95.2)	0.273
Dyslipidaemia	126 (87.5)	14 (66.7)	0.013
Chronic kidney disease	40 (27.8)	7 (33.3)	0.598
Left ventricular ejection fraction	59.3 ± 9.3	58.9 ± 11.6	0.895
Statin	118 (81.9)	13 (61.9)	0.034
Aspirin	137 (95.1)	20 (95.2)	0.600
Ticlopidine	25 (17.4)	2 (9.5)	0.554
Clopidogrel	114 (79.2)	18 (85.7)	0.683
Dual antiplatelet therapy	138 (95.8)	19 (90.5)	0.600
Bare-metal stent	27 (18.8)	3 (14.3)	0.847
Stent diameter (mm)	3.4 ± 0.3	3.3 ± 0.4	0.278
Total stent length (mm)	22.5 ± 9.6	25.4 ± 10.5	0.206
Chronic total occlusion	6 (4.2)	2 (9.5)	0.601
Stenosis severity	91.1 ± 9.2	89.4 ± 10.2	0.436
Distance between the ostium of the LAD and the proximal edge of the stent (mm)	5.2 ± 5.1	9.2 ± 6.3	0.002
Final minimum lumen diameter (mm)	3.0 ± 0.3	2.6 ± 0.6	0.004
High-degree calcification	11 (7.6)	4 (19.0)	0.196
Lesion length (mm)	17.8 ± 11.5	15.6 ± 10.6	0.411
Lesion angulation > 60°	4 (2.8)	0 (0)	0.989
Diagonal branch	83 (57.6)	13 (61.9)	0.711
Predilatation	118 (81.9)	18 (85.7)	0.907
Postdilatation	60 (41.7)	8 (38.1)	0.756
Kissing balloon technique	4 (2.8)	2 (9.5)	0.358
Intravascular ultrasound	137 (95.1)	19 (90.5)	0.715
Angles (deg.)			
Left main trunk–left anterior descending (Spider view)	32.0 ± 18.1	38.5 ± 18.5	0.121
Left main trunk–left circumflex (Spider view)	43.4 ± 20.7	39.7 ± 21.0	0.449
Left anterior descending–left circumflex (Spider view)	75.4 ± 24.5	78.2 ± 24.6	0.497
Left main trunk–left anterior descending (RAO/CAU view)	17.5 ± 10.1	27.3 ± 14.3	< 0.001

Values are means ± SD or numbers (%) of observations.
CAU, caudal; LAD, left anterior descending; RAO, right anterior oblique.

angle (Spider view) was similar in all groups, whereas the mean LAD–LCX angle (Spider view) was significantly wider in the in-stent restenosis than in the no-restenosis group. The mean LMT–LAD angle (RAO/CAU) was wider in both the in-stent and the in-segment restenosis groups than in the no-restenosis group.

Univariate and multivariate logistic regression analyses were carried out to determine independent predictors of each type of restenosis (Table 5). The administration of statin was related to dyslipidaemia and stent length was related to lesion length. Several factors influence the kissing balloon technique technique, including operator's proficiency, CKD, ST segment elevation myocardial infarction as an indication for PCI, a narrow bifurcation angle and stent platforms [17]. Therefore, we excluded statin administration, stent length and kissing balloon technique from the multivariate analysis.

Independent risk factors of total restenosis were distance between the ostium of the LAD and the proximal edge of the stent, final MLD and LMT–LAD angle (Spider view) (Table 5). Factors that were independently related to in-stent restenosis were final MLD, lesion length and LMT–LAD angle (Spider view) (Table 6). The distance between the ostium of the LAD artery and the proximal edge of the stent was an independent risk factor of in-segment restenosis (Table 7).

By multivariate analysis, the predictors of in-stent and in-segment restenosis were distance between the ostium of the LAD and the proximal edge of the stent, final MLD and LMT–LAD angle (RAO/CAU) (Table 8). Lesion length was an independent predictor of in-stent restenosis. LMT–LAD angle (RAO/CAU) was an independent predictor of in-segment restenosis, besides distance between ostium of the LAD and the proximal edge of the stent.

When we entered the LAD–LCX angle (Spider view) instead of the LMT–LAD angle (Spider view) in the multivariate analysis, significant predictors of in-stent and in-segment restenosis were (a) distance between ostium of the LAD and the proximal edge of the stent and (b) final MLD (Table 9). Although the LAD–LCX angle (Spider view) was a predictor of in-stent restenosis by univariate analysis, it was no longer statistically significant by multivariate analysis. The predictors of in-stent restenosis were final MLD and lesion length, and the predictor of in-segment restenosis was distance between the ostium of the LAD and the proximal edge of the stent (Table 9). These observations suggest that the LMT–LAD angle is a stronger predictor of restenosis after PCI for the pLAD artery than the LAD–LCX angle.

In this multivariate analysis, a greater than 34° LMT–LAD angle (Spider view), which was the mean angle among all patients, was associated with a risk of restenosis expressed as OR 3.48 (95% CI: 1.37–8.85; $P=0.009$) and a greater than 20° LMT–LAD angle (RAO/CAU), which was also the mean angle, was associated with a risk of restenosis expressed as OR 3.61 (95% CI: 1.43–9.10; $P=0.006$). A final MLD of less than 3.0 mm was associated with an OR 0.12 (95% CI: 0.02–0.87; $P=0.036$) and a lesion length of more than 18 mm with an OR 10.13 (95% CI: 1.53–66.96; $P=0.016$) for in-stent restenosis. A distance of more than 10 mm between the ostium of the LAD and the proximal edge of the stent was correlated strongly with in-segment restenosis (OR 7.97; 95% CI: 2.12–29.92; $P=0.002$).

Table 10 shows the patterns of stent restenosis and their mechanisms or causes in our study. Axial geographic miss (AGM) was observed in eight of 12 cases (67%) in the in-stent restenosis group, whereas in the in-segment restenosis group, longitudinal geographic miss (LGM) was observed in 20 of 21 cases (95%).

Table 5 Univariate and multivariate logistic regression analyses of total restenosis

	Analysis			
	Univariate OR (95% CI)	*P*	Multivariate OR (95% CI)	*P*
Male sex	1.39 (0.53–3.65)	0.659	1.94 (0.61–6.20)	0.263
Diabetes	1.89 (0.88–4.04)	0.147	1.27 (0.52–3.10)	0.600
Hypertension	1.45 (0.47–4.50)	0.703	1.65 (0.44–6.22)	0.457
Dyslipidaemia	0.38 (0.15–0.95)	0.062	0.51 (0.16–1.66)	0.513
Chronic kidney disease	1.92 (0.88–4.18)	0.150	1.60 (0.62–4.13)	0.336
Bare-metal stent	1.17 (0.46–2.97)	0.937	1.49 (0.46–4.79)	0.502
Chronic total occlusion	2.30 (0.54–9.72)	0.470	1.98 (0.35–11.1)	0.439
Distance between the ostium of the LAD and the proximal edge of the stent (mm)	3.10 (1.31–7.36)	0.017	4.91 (1.60–15.1)	0.006
Final MLD (mm)	0.24 (0.10–0.57)	0.001	0.26 (0.10–0.67)	0.006
High-degree calcification	2.69 (0.91–7.89)	0.127	1.19 (0.32–4.42)	0.799
Lesion length (mm)	1.30 (0.60–2.83)	0.647	1.63 (0.60–4.41)	0.339
Angle				
Left main trunk–left anterior descending (Spider view)	2.80 (1.26–6.21)	0.016	3.48 (1.37–8.85)	0.009
Left main trunk–left circumflex (Spider view)	0.85 (0.39–1.82)	0.816	1.55 (0.60–4.02)	0.371

There was no correlation ($r=-0.237$, $r^2=0.056$) between the LMT–LAD and LMT–LCX angles (Spider view). There was, however, a correlation ($r=0.626$, $r^2=0.392$) between the LMT–LAD and LAD–LCX angles (Spider view). Therefore, we excluded the LAD–LCX angle from the multivariate analysis when analysing the LMT–LAD angle (Spider view).

CI, confidence interval; LAD, left anterior descending; LCX, left circumflex; LMT, left main trunk; MLD, minimal lumen diameter; OR, odds ratio.

Table 6 Univariate and multivariate logistic regression analyses of in-stent restenosis

	Analysis			
	Univariate OR (95% CI)	*P*	Multivariate OR (95% CI)	*P*
Male sex	1.55 (0.32–7.40)	0.848	2.66 (0.36–19.8)	0.340
Diabetes	1.57 (0.48–5.11)	0.654	1.43 (0.30–6.72)	0.651
Hypertension	0.60 (0.15–2.38)	0.737	0.29 (0.04–1.91)	0.195
Dyslipidaemia	0.71 (0.14–3.53)	0.972	0.32 (0.03–3.09)	0.324
Chronic kidney disease	2.60 (0.79–8.53)	0.196	3.28 (0.57–19.0)	0.185
Bare-metal stent	2.17 (0.61–7.72)	0.401	2.76 (0.43–17.6)	0.284
Chronic total occlusion	2.09 (0.23–19.0)	0.955	1.74 (0.11–27.5)	0.695
Distance between the ostium of the LAD and the proximal stent (mm)	1.24 (0.25–6.08)	0.861	0.76 (0.08–7.53)	0.816
Final MLD (mm)	0.15 (0.03–0.72)	0.017	0.12 (0.02–0.87)	0.036
High-degree calcification	2.42 (0.47–12.4)	0.587	0.84 (0.10–7.00)	0.871
Lesion length (mm)	6.00 (1.55–23.1)	0.010	10.1 (1.53–66.9)	0.016
Angle				
Left main trunk–left anterior descending (Spider view)	7.00 (1.48–33.1)	0.013	7.63 (1.16–50.4)	0.035
Left main trunk–left circumflex (Spider view)	1.15 (0.35–3.73)	0.944	2.38 (0.46–12.4)	0.303

CI, confidence interval; LAD, left anterior descending; MLD, minimal lumen diameter; OR, odds ratio.

Table 7 Univariate and multivariate logistic regression analyses of in-segment restenosis

	Analysis			
	Univariate OR (95% CI)	*P*	Multivariate OR (95% CI)	*P*
Male sex	1.31 (0.41–4.17)	0.852	1.68 (0.40–7.14)	0.483
Diabetes	2.10 (0.83–5.29)	0.177	1.47 (0.50–4.32)	0.485
Hypertension	4.00 (0.51–31.2)	0.273	6.33 (0.61–65.6)	0.123
Dyslipidaemia	0.29 (0.10–0.80)	0.031	0.50 (0.13–1.86)	0.298
Chronic kidney disease	1.60 (0.62–4.15)	0.474	1.44 (0.44–4.76)	0.552
Bare-metal stent	0.72 (0.20–2.63)	0.847	0.94 (0.19–4.71)	0.938
Chronic total occlusion	2.42 (0.46–12.9)	0.600	4.30 (0.46–40.3)	0.201
Distance between the ostium of the LAD and the proximal stent (mm)	4.65 (1.74–12.5)	0.003	7.97 (2.12–29.9)	0.002
Final MLD (mm)	0.30 (0.11–0.82)	0.028	3.11 (0.97–9.97)	0.056
High-degree calcification	2.84 (0.81–9.94)	0.196	1.56 (0.33–7.37)	0.572
Lesion length (mm)	0.47 (0.15–1.48)	0.287	0.55 (0.13–2.40)	0.426
Angle				
Left main trunk–left anterior descending (Spider view)	1.87 (0.74–4.71)	0.271	2.39 (0.78–7.34)	0.130
Left main trunk–left circumflex (Spider view)	0.80 (0.32–1.98)	0.793	1.58 (0.46–5.36)	0.467

CI, confidence interval; LAD, left anterior descending; MLD, minimal lumen diameter; OR, odds ratio.

Table 8 Multivariate logistic regression analysis of total, in-stent and in-segment restenosis, including the left main trunk–left anterior descending angle (RAO/CAU)

	Total restenosis		In-stent restenosis		In-segment restenosis	
	OR (95% CI)	*P*	OR (95% CI)	*P*	OR (95% CI)	*P*
Male sex	1.51 (0.49–4.65)	0.472	2.32 (0.31–17.5)	0.411	1.31 (0.32–5.46)	0.707
Diabetes	1.44 (0.59–3.49)	0.422	2.11 (0.43–10.4)	0.359	1.48 (0.50–4.35)	0.476
Hypertension	1.93 (0.50–7.55)	0.344	0.39 (0.06–2.37)	0.308	9.50 (0.75–120)	0.082
Dyslipidaemia	0.54 (0.17–1.72)	0.294	0.32 (0.03–3.02)	0.317	0.48 (0.13–1.83)	0.513
Chronic kidney disease	1.73 (0.67–4.46)	0.258	2.46 (0.45–13.6)	0.302	1.75 (0.52–5.91)	0.370
Bare-metal stent	1.50 (0.48–4.70)	0.485	4.89 (0.77–31.0)	0.092	0.88 (0.18–4.39)	0.874
Chronic total occlusion	2.11 (0.36–12.5)	0.410	1.48 (0.10–23.0)	0.782	4.63 (0.47–45.2)	0.188
Distance between the ostium of LAD and the proximal edge of the stent (mm)	3.58 (1.21–10.6)	0.021	0.44 (0.04–4.43)	0.482	6.37 (1.69–24.0)	0.006
Final minimum lumen diameter (mm)	0.28 (0.11–0.73)	0.009	0.17 (0.03–1.04)	0.056	0.31 (0.09–1.03)	0.056
High-degree calcification	1.48 (0.40–5.43)	0.556	2.34 (0.31–17.7)	0.412	1.52 (0.31–7.47)	0.604
Lesion length (mm)	1.59 (0.58–4.36)	0.368	13.1 (1.70–101)	0.014	0.52 (0.12–2.30)	0.387
Angle						
Left main trunk–left circumflex (Spider view)	0.85 (0.39–1.82)	0.816	2.12 (0.39–11.6)	0.386	1.11 (0.30–4.10)	0.878
Left main trunk–left anterior descending (RAO/CAU)	3.61 (1.43–9.10)	0.006	4.73 (1.00–22.5)	0.051	3.83 (1.20–12.2)	0.024

There was no correlation ($r = -0.180$, $r^2 = 0.032$) between the LMT–LCX angle (Spider view) and the LMT–LAD angle (RAO/CAU view).
CAU, caudal; CI, confidence interval; LAD, left anterior descending; LCX, left circumflex; LMT, left main trunk; MLD, minimal lumen diameter; OR, odds ratio; RAO, right anterior oblique.

Table 9 Multivariate logistic regression analysis of total, in-stent and in-segment restenosis, including the left anterior descending–left circumflex angle

	Total restenosis		In-stent restenosis		In-segment restenosis	
	OR (95% CI)	*P*	OR (95% CI)	*P*	OR (95% CI)	*P*
Male sex	1.46 (0.48–4.42)	0.502	1.82 (0.26–12.8)	0.550	1.25 (0.32–4.96)	0.748
Diabetes	1.22 (0.51–2.93)	0.662	1.45 (0.33–6.43)	0.621	1.39 (0.48–4.06)	0.544
Hypertension	1.78 (0.50–6.32)	0.374	0.41 (0.07–2.43)	0.324	6.49 (0.66–63.8)	0.109
Dyslipidaemia	0.65 (0.21–1.98)	0.449	0.37 (0.05–2.99)	0.353	0.59 (0.16–2.15)	0.425
Chronic kidney disease	2.03 (0.78–5.29)	0.146	2.22 (0.45–10.9)	0.327	1.93 (0.57–6.55)	0.294
Bare-metal stent	1.42 (0.47–4.28)	0.537	2.93 (0.53–16.3)	0.220	0.90 (0.19–4.28)	0.898
Chronic total occlusion	2.05 (0.38–11.1)	0.406	1.10 (0.08–15.8)	0.943	5.23 (0.60–45.4)	0.133
Distance between the ostium of LAD and the proximal edge of the stent (mm)	3.26 (1.18–9.02)	0.023	0.68 (0.08–5.68)	0.723	5.46 (1.70–17.6)	0.004
Final MLD (mm)	0.27 (0.10–0.69)	0.006	0.15 (0.03–0.85)	0.032	0.34 (0.11–1.08)	0.066
High-degree calcification	1.38 (0.38–4.99)	0.620	1.56 (0.21–11.4)	0.662	1.67 (0.35–7.89)	0.515
Lesion length (mm)	1.37 (0.52–3.58)	0.527	7.88 (1.37–45.2)	0.021	0.45 (0.11–1.92)	0.283
Angle						
Left anterior descending–left circumflex (Spider view)	2.41 (0.99–5.85)	0.053	3.16 (0.69–14.4)	0.137	1.97 (0.65–5.96)	0.231

CI, confidence interval; LAD, left anterior descending; MLD, minimal lumen diameter; OR, odds ratio.

Discussion

The major observations made in this study were as follows: (i) the final MLD, lesion length and LMT–LAD angle were predictors of in-stent restenosis after PCI for pLAD artery disease and (ii) the distance between the ostium of the LAD and the proximal edge of the stent and the LMT–LAD angle were predictors of in-segment restenosis. To the best of our knowledge, this study is the first to (a) show a correlation between the LMT–LAD angle and restenosis in the pLAD artery and (b) compare the LMT–LAD angle with other predictors of restenosis by multivariate analysis. It contributes important anatomical information towards the list of clinical, procedural and angiographic predictors of outcome after PCI for the pLAD artery.

The incidence of stent restenosis after PCI for pLAD artery disease published in the past 10–15 years varies between 4.1 and 24.3% [18–24]. It remains the most common complication of PCI and a major clinical challenge. As the LMT–LAD angle provides unique information on stented coronary arteries, we hypothesized that it would yield additional anatomical characteristics associated with the incidence of restenosis after implantation of stents in the pLAD.

Comparison with previous measurements of angulation

Our measurements are concordant with the average bifurcation angles reported in previous studies. In this study, the average LMT–LAD, LAD–LCX and LMT–LCX angles in the Spider view measured $34.1° \pm 18.5°$, $75.6° \pm 24.5°$ and $42.8° \pm 20.1°$, respectively. Using 64-multislice computed angiographic tomography, Kawasaki *et al.* [25] reported LMT–LAD, LAD–LCX and LMT–LCX angles averaging $37° \pm 13°$, $72° \pm 22°$ and $59° \pm 21°$, respectively, and Rodriguez-Granillo *et al.* [26] reported a median LAD–LCX angle of 88.5°. In 100 patients with suspected coronary artery disease, Pflederer

Table 10 Patterns and mechanisms of restenosis

	Restenosis		Longitudinal geographic miss		Axial geographic miss	
Patient number	In-stent	In-segment	Balloon injury	Uncovered plaque	Oversizing	Undersizing
1	Focal (proximal)		1	1	1	
2	Focal (proximal)					1
3	Intrastent (proximal)					1
4	Focal (proximal)			1		1
5	Focal (proximal)		1			
6	Focal (proximal)			1		1
7	Intrastent (diffuse)			1		
8	Focal (proximal)			1		
9	Focal (proximal)					1
10	Focal (distal)					1
11	Focal (proximal)					1
12	Focal (proximal)			1		
13		Proximal	1	1	1	
14		Distal				1
15		Proximal	1			
16		Proximal	1	1		
17		Proximal		1		
18		Proximal		1		
19		Proximal		1		
20		Proximal		1	1	
21		Proximal		1		
22		Distal	1	1		
23		Proximal		1	1	
24		Proximal		1	1	
25		Proximal		1	1	
26		Proximal		1	1	
27		Proximal	1	1	1	
28		Proximal		1	1	
29		Proximal		1	1	
30		Proximal	1	1		
31		Proximal		1	1	
32		Proximal		1		
33		Proximal		1		

et al. [27] reported an average LAD–LCX angle of $80 \pm 27°$, and in a postmortem study of 100 human hearts, Reig and Petit [28] reported an average LAD–LCX angle of $86.7° \pm 28.8°$. Although there might be an inherent discrepancy between values measured by two-dimensional coronary angiogram and the real angles in the three-dimensional space, our data measured in the Spider view are similar to those reported by previous studies.

A wide angulation causes low wall shear stress, atherosclerosis and restenosis

In wide-angled models, large areas of low wall shear stress (WSS) have been observed, particularly in the bifurcation region, which were not present in narrow-angled models [26,29]. In simulated and actual computed tomography (CT) images, Chaichana *et al.* [29] studied the haemodynamic effects of various angulations of the left coronary artery, and found a direct relationship between the LAD–LCX angle and haemodynamic changes. A low WSS and stress gradient were observed with LAD–LCX angles between 75° and 120° compared with LAD–LCX angles models between 15° and 60°. Some studies observed that wider LAD–LCX angles were prone to atherosclerotic progression at the site of bifurcation. Using CT coronary angiography, Sun and Cao [30] examined 30 patients suspected of having coronary artery disease and measured a mean LAD–LCX angle of $75.5° \pm 19.8°$ in patients with normal versus $94° \pm 19.7°$ in patients with diseased left coronary arteries ($P = 0.02$). Using high-resolution multislice CT coronary angiography, Rodriguez-Granillo *et al.* [26] observed that the median LAD–LCX angle was 88.5°, and that 72% of normal vessels had an angle of less than 88.5°, whereas 63% of diseased vessels had an LAD–LCX angle of at least 88.5° ($P = 0.018$). In our study, the average $84.0° \pm 23.6°$ of the LAD–LCX angle measured in the Spider view among patients with restenosis was significantly wider ($P = 0.040$) than the $75.4° \pm 24.5°$ measured in patients without restenosis. When we used the mean 76° as the cut-off LAD–LCX angle in the univariate analysis, the LAD–LCX angle emerged as a significant predictor of total restenosis (OR, 2.45; 95% CI: 1.12–5.36; $P = 0.037$). However, by multivariate analysis, the LAD–LCX angle lost its statistical significance (Table 9). In contrast, when we used 34° as the cut-off value for the LMT–LAD angle, its statistical significance was preserved, even after adjustments for confounding factors, suggesting that (a) the LMT–LAD angle is a more reliable predictor of pLAD artery restenosis than the LAD–LCX angle and (b) a wider LMT–LAD angle is more closely associated with restenosis after stent

implantation for pLAD artery disease than a narrower angle. As for LMT–LAD cross-over single stenting, Amemiya *et al.* [31] also reported that the wide LMT–LAD angle group (>52°) had a higher rate of target lesion revascularization than the narrower angle group.

Mechanisms of proximal LAD artery restenosis

Wide angulation

A wide bifurcation angle causes high turbulence and low WSS, which might promote plaque proliferation in bifurcated regions [26,29,30,32–34]. A low WSS causes abnormal biochemical responses, such as the expression of adhesion molecules, weakening of cell junctions, monocyte deposition, increased permeability to lipids and macrophages and smooth muscle cell proliferation [35,36]. This inverse correlation between neointimal proliferation and WSS was observed in both in-stent segments and at the edges of the stent [37].

Geographic miss

Costa *et al.* [15] evaluated the clinical impact of stent deployment techniques and found that geographic miss was an independent clinical or anatomic risk factor for restenosis and target vessel revascularization. In that study, LGM was defined as an injured or diseased stenotic segment not completely covered by the stent and AGM was defined as potential undersizing or oversizing of the balloon. The patterns of restenosis were classified as (a) focal when length was less than 10 mm, (b) diffuse when restenosis was more than 10 mm inside the stent, (c) proliferative when restenosis was more than 10 mm in length and extending outside the stent and (d) occlusive [38]. Table 10 shows that AGM was observed more in the in-stent restenosis group, whereas in the in-segment restenosis group, LGM was commonly observed. These observations suggest that in-stent restenosis is likely to be induced by AGM, whereas in-segment restenosis is mainly caused by LGM. Both types of geographic miss were often caused by iatrogenic or periprocedural adverse events.

The longer the distance between the ostium of the LAD and the proximal edge of the stent in this study, the higher the incidence of restenosis, particularly in-segment restenosis. One might hypothesize that the longer the distance from the ostium of the LAD artery, the higher the likelihood of LGM (caused by, for example, uncovered plaque or balloon injury), which could promote in-segment restenosis, although the relationship between in-segment restenosis and distance from the ostium of the LAD remains controversial.

Coronary artery movement

Konta and Bett [39] studied the relationship between coronary artery movement and mechanical stress, which may lead to the development of atherosclerosis. They found that the compression type of coronary artery movement might play an important role in the progression of coronary artery atherosclerosis and that the pLAD artery was one of the segments where the compressive movement was exerted in the longitudinal direction. During the cardiac cycle, injured or diseased pLAD segments with residual plaques not covered by the stent (LGM) are likely to be exposed to the incessant injuries caused by the edge of the stent because of the compression movement of pLAD artery, which might result in an edge vascular response. Therefore, LGM causes mainly in-segment restenosis and only limited in-stent restenosis (Table 10).

Restenosis in the proximal segment

Several studies have reported a higher incidence of restenosis in the proximal than in the distal segments of the stents [40–42]. In this study, both in-stent and in-segment restenosis were likely to occur in the proximal segment of the implanted stent (Table 10). In the in-stent restenosis group, restenosis occurred in the proximal body of a stent in 10 of 12 patients, whereas in the in-segment restenosis group, restenosis was observed in the proximal segment in 19 of 21 patients. These observations support the hypothesis that a wide LMT–LAD angle, which leads to a wide range of low wall shear stress caused by the disturbances of bloodstream in the pLAD artery, plays an important role in the development of restenosis after the treatment of pLAD artery disease, besides geographic miss and coronary artery movement as mechanical risk factors of restenosis, combined with metabolic factors such as diabetes, hypertension and dyslipidaemia.

Other observations

In this study, dyslipidaemia was more prevalent in the no-restenosis group than in the restenosis group by univariate analysis. This result might seem inconsistent as disorders of the lipid metabolism are considered a risk factor for restenosis. However, the high rate of statin administration in this study might explain this discrepancy. Some studies have shown that the administration of statin can cause a significant regression of the coronary plaque volume and is effective in the secondary prevention of coronary artery disease [43,44]. Statins were administered in 93.7% of patients with abnormal lipids in the no-restenosis group versus 91.7% in the restenosis group (NS).

Although diabetes is a well-known predictor of restenosis after stent implantation, it was not a significant risk factor in this study. This discrepancy was explained by a high rate of diabetes control. The mean plasma haemoglobin A1c in the in-stent restenosis group was 6.7 ± 1.2 versus 6.5 ± 0.4% in the in-segment restenosis group.

Limitations of our study

The sample size of this retrospective, observational study, carried out at a single medical centre, was small. Its results need to be confirmed prospectively in a larger multiple-centre study. Second, we analysed lesion length, final MLD and the distance between the ostium of the LAD and the proximal edge of the stent by QCA because some of the intravascular ultrasound data were missing and unavailable. Our results, therefore, should be confirmed by intravascular ultrasound in a future study. Third, as the angles measured by two-dimensional QCA were not always actual angles, we should also confirm our results by reconstruction of the images on three-dimensional QCA or computed tomography. The reason why we selected two-dimensional QCA in this study was that the three-dimensional QCA system was available only in limited facilities.

Clinical implications

Despite these limitations, our study showed that, among several risk factors associated with restenosis of the pLAD artery, patients with a wide LMT–LAD angle were at a higher risk. The LMT–LAD angle provides clinically important information towards the prevention of restenosis as patients with a wide angle should receive more intensive treatments of other risk factors. The distance between the ostium of the LAD and the proximal edge of the stent should be short to completely cover a residual plaque or vascular segment injured by a balloon.

Conclusion

The results of this study suggest that a wide LMT–LAD angle is associated with a higher risk of restenosis after stent implantation for pLAD artery disease.

Acknowledgements

The authors appreciate the excellent support of the staff in the catheterization laboratory at Hokkaido Cardiovascular Hospital during this study.

Conflicts of interest

There are no conflicts of interest.

Appendix

Factors chosen as potential factors of risk of restenosis:

Age

Sex

Canadian Cardiovascular Society classification

Acute coronary syndrome

Diabetes mellitus

Hypertension

Dyslipidaemia

Chronic kidney disease

Left ventricular ejection fraction

Angle between:

(1) the left main trunk and the left anterior descending artery in
   (a) the left anterior oblique/caudal ('Spider view') and
   (b) the right anterior oblique/caudal (RAO/CAU) view
(2) the left anterior descending and the left circumflex artery in Spider view
(3) the left main trunk and the left circumflex artery in Spider view

Stent

Diameter

Length

Type

Chronic total occlusion

Stenosis severity

Distance between the ostial left anterior descending and the proximal edge of the stent

Final minimum lumen diameter

Lesion length

Diagonal branch

Kissing balloon technique

Predilatation

Postdilatation

Intravascular ultrasound

References

1 Klein LW, Weintraub WS, Agarwal JB, Schneider RM, Seelaus PA, Katz RI, Helfant RH. Prognostic significance of severe narrowing of the proximal portion of the left anterior descending coronary artery. *Am J Cardiol* 1986; **58**:42–46.

2 Mahmarian JJ, Pratt CM, Boyce TM, Verani MS. The variable extent of jeopardized myocardium in patients with single vessel coronary artery disease: quantification by thallium-201 single photon emission computed tomography. *J Am Coll Cardiol* 1991; **17**:355–362.

3 Calais F, Lagerqvist B, Leppert J, James SK, Fröbert O. Proximal coronary artery intervention: stent thrombosis, restenosis and death. *Int J Cardiol* 2013; **170**:227–232.

4 Lemos PA, Hoye A, Goedhart D, Arampatzis CA, Saia F, van der Giessen WJ, *et al.* Clinical, angiographic, and procedural predictors of angiographic restenosis after sirolimus-eluting stent implantation in complex patients: an evaluation from the Rapamycin-Eluting Stent Evaluated At Rotterdam Cardiology Hospital (RESEARCH) study. *Circulation* 2004; **109**:1366–1370.

5 Roy P, Okabe T, Pinto Slottow TL, Steinberg DH, Smith K, Torguson R, *et al.* Correlates of clinical restenosis following intracoronary implantation of drug-eluting stents. *Am J Cardiol* 2007; **100**:965–969.

6 Blazek S, Holzhey D, Jungert C, Borger MA, Fuernau G, Desch S, *et al.* Comparison of bare-metal stenting with minimally invasive bypass surgery for

stenosis of the left anterior descending coronary artery: 10-year follow-up of a randomized trial. *JACC Cardiovasc Interv* 2013; **6**:20–26.
7 Serruys PW, Morice MC, Kappetein AP, Colombo A, Holmes DR, Mack MJ, *et al*. Percutaneous coronary intervention versus coronary-artery bypass grafting for severe coronary artery disease. *N Engl J Med* 2009; **360**:961–972.
8 Etienne PY, D'hoore W, Papadatos S, Mairy Y, El Khoury G, Noirhomme P, *et al*. Five-year follow-up of drug-eluting stents implantation vs minimally invasive direct coronary artery bypass for left anterior descending artery disease: a propensity score analysis. *Eur J Cardiothorac Surg* 2013; **44**:884–890.
9 Thiele H, Oettel S, Jacobs S, Hambrecht R, Sick P, Gummert JF, *et al*. Comparison of bare-metal stenting with minimally invasive bypass surgery for stenosis of the left anterior descending coronary artery: a 5-year follow-up. *Circulation* 2005; **112**:3445–3450.
10 Goy JJ, Kaufmann U, Hurni M, Cook S, Versaci F, Ruchat P, *et al*. 10-year follow-up of a prospective randomized trial comparing bare-metal stenting with internal mammary artery grafting for proximal, isolated de novo left anterior coronary artery stenosis the SIMA (Stenting versus Internal Mammary Artery grafting) trial. *J Am Coll Cardiol* 2008; **52**:815–817.
11 Thiele H, Neumann-Schniedewind P, Jacobs S, Boudriot E, Walther T, Mohr FW, *et al*. Randomized comparison of minimally invasive direct coronary artery bypass surgery versus sirolimus-eluting stenting in isolated proximal left anterior descending coronary artery stenosis. *J Am Coll Cardiol* 2009; **53**:2324–2331.
12 Kapoor JR, Gienger AL, Ardehali R, Varghese R, Perez MV, Sundaram V, *et al*. Isolated disease of the proximal left anterior descending artery comparing the effectiveness of percutaneous coronary interventions and coronary artery bypass surgery. *JACC Cardiovasc Interv* 2008; **1**:483–491.
13 Levine GN, Bates ER, Blankenship JC, Bailey SR, Bittl JA, Cercek B, *et al*. 2011 ACCF/AHA/SCAI guideline for percutaneous coronary intervention: executive summary: a report of the American College of Cardiology Foundation/American Heart Association Task Force on Practice Guidelines and the Society for Cardiovascular Angiography and Interventions. *Circulation* 2011; **124**:2574–2609.
14 Hong SJ, Kim MH, Ahn TH, Ahn YK, Bae JH, Shim WJ, *et al*. Multiple predictors of coronary restenosis after drug-eluting stent implantation in patients with diabetes. *Heart* 2006; **92**:1119–1124.
15 Costa MA, Angiolillo DJ, Tannenbaum M, Driesman M, Chu A, Patterson J, *et al*. Impact of stent deployment procedural factors on long-term effectiveness and safety of sirolimus-eluting stents (final results of the multicenter prospective STLLR trial). *Am J Cardiol* 2008; **101**:1704–1711.
16 Tu S, Jing J, Holm NR, Onsea K, Zhang T, Adriaenssens T, *et al*. In vivo assessment of bifurcation optimal viewing angles and bifurcation angles by three-dimensional (3D) quantitative coronary angiography. *Int J Cardiovasc Imaging* 2012; **28**:1617–1625.
17 Grundeken MJ, Lesiak M, Asgedom S, Garcia E, Bethencourt A, Norell MS, *et al*. Clinical outcomes after final kissing balloon inflation compared with no final kissing balloon inflation in bifurcation lesions treated with a dedicated coronary bifurcation stent. *Heart* 2014; **100**:479–486.
18 Guardado JH, Moreno R, Costa J, Perez-Viscayno MJ, Segura L, Alfonso F, *et al*. Proximal left anterior descending coronary artery revascularization with drug-eluting stents. *Arq Bras Cardiol* 2007; **88**:159–166.
19 Seung KB, Kim YH, Park DW, Lee BK, Lee CW, Hong MK, *et al*. Effectiveness of sirolimus-eluting stent implantation for the treatment of ostial left anterior descending artery stenosis with intravascular ultrasound guidance. *J Am Coll Cardiol* 2005; **46**:787–792.
20 Valencia J, Berenguer A, Mainar V, Bordes P, Gómez S, Tello A, *et al*. Two-year follow-up of sirolimus-eluting stents for the treatment of proximal left anterior descending coronary artery stenosis. *J Interv Cardiol* 2006; **19**:126–134.
21 Golmohammadia Z, Sokhanvar S, Aslanabadia N, Ghaffaria S, Sohrabia B. One-year outcomes after everolimus-eluting stents implantation in ostial lesions of left anterior descending coronary arteries. *Cardiol Res* 2013; **4**:192–198.
22 Drenth DJ, Veeger NJ, Winter JB, Grandjean JG, Mariani MA, van Boven AJ, Boonstra PW. A prospective randomized trial comparing stenting with off-pump coronary surgery for high-grade stenosis in the proximal left anterior descending coronary artery: three-year follow-up. *J Am Coll Cardiol* 2002; **40**:1955–1960.
23 Versaci F, Gaspardone A, Tomai F, Proietti I, Ghini AS, Altamura L, *et al*. A comparison of coronary artery stenting with angioplasty for isolated stenosis of the proximal left anterior descending coronary artery: five year clinical follow up. *Heart* 2004; **90**:672–675.
24 Diegeler A, Spyrantis N, Matin M, Falk V, Hambrecht R, Autschbach R, *et al*. The revival of surgical treatment for isolated proximal high grade LAD lesions by minimally invasive coronary artery bypass grafting. *Eur J Cardiothorac Surg* 2000; **17**:501–504.
25 Kawasaki T, Koga H, Serikawa T, Orita Y, Ikeda S, Mito T, *et al*. The bifurcation study using 64 multislice computed tomography. *Catheter Cardiovasc Interv* 2009; **73**:653–658.
26 Rodriguez-Granillo GA, Rosales MA, Degrossi E, Durbano I, Rodriguez AE. Multislice CT coronary angiography for the detection of burden, morphology and distribution of atherosclerotic plaques in the left main bifurcation. *Int J Cardiovasc Imaging* 2007; **23**:389–392.
27 Pflederer T, Ludwig J, Ropers D, Daniel WG, Achenbach S. Measurement of coronary artery bifurcation angles by multidetector computed tomography. *Invest Radiol* 2006; **41**:793–798.
28 Reig J, Petit M. Main trunk of the left coronary artery: anatomic study of the parameters of clinical interest. *Clin Anat* 2004; **17**:6–13.
29 Chaichana T, Sun Z, Jewkes J. Computation of hemodynamics in the left coronary artery with variable angulations. *J Biomech* 2011; **44**:1869–1878.
30 Sun Z, Cao Y. Multislice CT angiography assessment of left coronary artery: correlation between bifurcation angle and dimensions and development of coronary artery disease. *Eur J Radiol* 2011; **79**:e90–e95.
31 Amemiya K, Domei T, Iwabuchi M, Shirai S, Ando K, Goya M, *et al*. Impact of the bifurcation angle on major cardiac events after cross-over single stent strategy in unprotected left main bifurcation lesions: 3-dimensional quantitative coronary angiographic analysis. *Am J Cardiovasc Dis* 2014; **4**:168–176.
32 Han SH, Puma J, García-García HM, Nasu K, Margolis P, Leon MB, Lerman A. Tissue characterisation of atherosclerotic plaque in coronary artery bifurcations: an intravascular ultrasound radiofrequency data analysis in humans. *EuroIntervention* 2010; **6**:313–320.
33 Gijsen FJ, Wentzel JJ, Thury A, Lamers B, Schuurbiers JC, Serruys PW, van der Steen AF. A new imaging technique to study 3-D plaque and shear stress distribution in human coronary artery bifurcations in vivo. *J Biomech* 2007; **40**:2349–2357.
34 Cecchi E, Giglioli C, Valente S, Lazzeri C, Gensini GF, Abbate R, Mannini L. Role of hemodynamic shear stress in cardiovascular disease. *Atherosclerosis* 2011; **214**:249–256.
35 Chappell DC, Varner SE, Nerem RM, Medford RM, Alexander RW. Oscillatory shear stress stimulates adhesion molecule expression in cultured human endothelium. *Circ Res* 1998; **82**:532–539.
36 VanderLaan PA, Reardon CA, Getz GS. Site specificity of atherosclerosis: site-selective responses to atherosclerotic modulators. *Arterioscler Thromb Vasc Biol* 2004; **24**:12–22.
37 Mongrain R, Rodés-Cabau J. Role of shear stress in atherosclerosis and restenosis after coronary stent implantation. *Rev Esp Cardiol* 2006; **59**:1–4.
38 Mehran R, Dangas G, Abizaid AS, Mintz GS, Lansky AJ, Satler LF, *et al*. Angiographic patterns of in-stent restenosis: classification and implications for long-term outcome. *Circulation* 1999; **100**:1872–1878.
39 Konta T, Bett JH. Patterns of coronary artery movement and the development of coronary atherosclerosis. *Circ J* 2003; **67**:846–850.
40 Moses JW, Leon MB, Popma JJ, Fitzgerald PJ, Holmes DR, O'Shaughnessy C, *et al*. Sirolimus-eluting stents versus standard stents in patients with stenosis in a native coronary artery. *N Engl J Med* 2003; **349**:1315–1323.
41 Shimohama T, Ako J, Yamasaki M, Otake H, Tsujino I, Hasegawa T, *et al*. SPIRIT III JAPAN versus SPIRIT III USA: a comparative intravascular ultrasound analysis of the everolimus-eluting stent. *Am J Cardiol* 2010; **106**:13–17.
42 Lemos PA, Saia F, Ligthart JM, Arampatzis CA, Sianos G, Tanabe K, *et al*. Coronary restenosis after sirolimus-eluting stent implantation: morphological description and mechanistic analysis from a consecutive series of cases. *Circulation* 2003; **108**:257–260.
43 Nissen SE, Nicholls SJ, Sipahi I, Libby P, Raichlen JS, Ballantyne CM, *et al*. Effect of very high-intensity statin therapy on regression of coronary atherosclerosis: the ASTEROID trial. *JAMA* 2006; **295**:1556–1565.
44 Takayama T, Hiro T, Yamagishi M, Daida H, Hirayama A, Saito S, *et al*. Effect of rosuvastatin on coronary atheroma in stable coronary artery disease: multicenter coronary atherosclerosis study measuring effects of rosuvastatin using intravascular ultrasound in Japanese subjects (COSMOS). *Circ J* 2009; **73**:2110–2117.